Design and Energetic Characterization of a Liquid-Propellant-Powered Actuator for Self-Powered Robots

Michael Goldfarb, *Member, IEEE*, Eric J. Barth, *Member, IEEE*, Michael A. Gogola, and Joseph A. Wehrmeyer

***Abstract*—This paper describes the design of a power supply and actuation system appropriate for position or force controlled human-scale robots. The proposed approach utilizes a liquid monopropellant to generate hot gas, which is utilized to power a pneumatic-type actuation system. A prototype of the actuation system is described, and closed-loop tracking data are shown, which demonstrate good motion control. Experiments to characterize the energetic performance of a six-degree-of-freedom actuation system indicate that the proposed system with a diluted propellant offers an energetic figure of merit five times greater than battery-powered dc motors. Projections based on these experiments indicate that the same system powered by undiluted propellant would offer an energetic figure of merit an order of magnitude greater than a comparable battery-powered dc motor actuated system.**

***Index Terms*—Actuators, actuation, energy density, human-scale robot, hydrogen peroxide, monopropellant, pneumatic, power supply, self-powered robot, service robot.**

I. Introduction

A. Motivation

ONE OF THE most significant challenges in the development of an autonomous human-scale robot is the issue of power supply. Perhaps the most likely power supply/actuator candidate system for a position or force actuated human-scale robot is an electrochemical battery and dc motor combination. This type of system, however, would have to carry an inordinate amount of battery weight in order to perform a significant amount of work for a significant period of time. A state-of-the-art example of a human-scale robot that utilizes electrochemical batteries combined with dc motor/harmonic drive actuators is the Honda Motor Corporation humanoid robot model P3. The P3 robot has a total mass of 130 kg (285 lb), 30 kg (66 lbs) of which are nickel-zinc batteries. These 30 kg of batteries provide sufficient power for approximately 15–25 min of operation, depending on its workload. Operation times of this magnitude are common in self-powered position or force controlled human-scale robots, and represent a major technological roadblock for designing actuated mobile robots that can operate power-autonomously for extended periods of time.

Manuscript received August 1, 2002; revised January 20, 2003.This work was supported in part by the U.S. Department of Defense, DARPA, under Grant DAAD190110509. Recommended by Guest Editors C. Mavroidis, E. Papadopoulos, and N. Sarkar.

M. Goldfarb, E. J. Barth, and J. A. Wehrmeyer are with the Department of Mechanical Engineering, Vanderbilt University, Nashville, TN 37235 USA (e-mail: goldfarb@vuse.vanderbilt.edu; barthej@vuse.vanderbilt.edu; wehrmeyer@vuse.vanderbilt.edu).

M. A. Gogola is with the MWD Engineering Department, Baker Hughes INTEQ, Houston, TX 77073 USA (e-mail: michael.gogola@bakeratlas.com).

Digital Object Identifier 10.1109/TMECH.2003.812842

B. Figure of Merit

Assuming that a given power supply and actuation system can deliver the requisite average and peak output power at a bandwidth required by a power-autonomous robot, three parameters are of primary interest in providing optimal energetic performance. These are the mass-specific energy density of the power source e_s, the efficiency of converting energy from the power source to controlled mechanical work η, and the maximum mass-specific power density of the energy conversion and/or actuation system p_a. A simple performance index is proposed by forming the product of these parameters

$$A_p = e_s \eta p_a \tag{1}$$

where A_p is called the actuation potential. Such a figure of merit is justified by the fact that a system with high power-source energy density, high conversion efficiency, and high actuator power density will be the lightest possible system capable of delivering a given amount of power and energy. In the case of a battery-powered dc-motor-actuated robot, the energy density of the power source e_s would be the electrical energy density of the battery, the conversion efficiency η would be the combined efficiency of the (closed-loop controlled) dc motor and gearhead, and the power density of the energy conversion and actuation system p_a would be the rated output power of the motor/gearhead divided by its mass. In the case of a gasoline-engine-powered hydraulically actuated system, the energy density of the power source would be the thermodynamic energy density of gasoline; the conversion efficiency would be the combined efficiency of the internal combustion engine (converting thermodynamic energy to shaft energy), hydraulic pump (converting shaft energy to hydraulic energy), and the hydraulic actuation system (converting hydraulic energy to controlled mechanical work); and finally, the power density of the energy conversion and actuation system would be the maximum output power of the hydraulic actuation system, divided by the combined mass of the engine, pump, accumulator, valves, cylinders, reservoir, and hydraulic fluid of the hydraulic system. With regard to this figure of merit, batteries and dc motors capable of providing the requisite power for a human-scale robot offer a reasonable conversion efficiency, but provide

relatively low power-source energy density and a similarly low actuator/gearhead power density. A gasoline-engine-powered hydraulically-actuated human-scale robot would provide a high power-source energy density, but a relatively low conversion efficiency and actuation system power density.

C. A Monopropellant Powered Approach

Liquid chemical fuels can provide energy densities significantly greater than power-comparable electrochemical batteries. The energy from these fuels, however, is released as heat, and the systems required to convert heat into controlled, actuated work are typically complex, heavy, and inefficient. One means of converting chemical energy into controlled, actuated work with a simple conversion process is to utilize a liquid monopropellant to generate a gas, which in turn can be utilized to power a pneumatic actuation system. Specifically, monopropellants are a class of fuels (technically propellants since oxidation does not occur) that rapidly decompose (or chemically react) in the presence of a catalytic material. Unlike combustion reactions, no ignition is required, and therefore the release of power can be controlled continuously and proportionally simply by controlling the flow rate of the liquid propellant. This results in a simple, low-weight energy converter system, which provides a good solution to the design tradeoffs between fuel energy density and system weight for the scale of interest.

Monopropellants, originally developed in Germany during World War II, have since been utilized in several applications involving power and propulsion, most notably to power gas turbine and rocket engines for underwater and aerospace vehicles. Modern day applications include torpedo propulsion, reaction control thrusters on a multitude of space vehicles, and auxiliary power turbo pumps for aerospace vehicles. Despite the use of monopropellants in these various applications, the authors have not been able to find any prior literature describing the development of position or force controllable monopropellant-powered actuators. The only indication of prior related work is the patent by Morash [1], which describes a pilot-operated binary valve that utilizes a monopropellant in the pilot stream. The work reported here describes the design of a monopropellant-powered actuation system appropriate for human-scale self-powered robots, and presents theoretical and experimental results that indicate the strong potential of this system for high energy density human-scale robot applications. Specifically, with regard to the figure of merit described by (1), the proposed approach is projected to provide a significantly greater power-source energy density and actuation power density relative to batteries and dc motors, and is projected to provide a higher conversion efficiency and significantly greater actuation system power density relative to a gasoline-powered hydraulic system.

II. Description of Monopropellant Actuation System

The monopropellant-powered actuation system is similar in several respects to a typical pneumatically actuated system, but rather than utilize a compressor to maintain a high-pressure reservoir, the proposed system utilizes the decomposition of hydrogen peroxide (H_2O_2) to pressurize a reservoir. Specifically, peroxide decomposes upon contact with a catalyst. This decomposition is a strongly exothermic reaction that produces water and oxygen in addition to heat. The heat, in turn, vaporizes the water and expands the resulting gaseous mixture of steam and oxygen. Since the liquid peroxide is stored at a high pressure, the resulting gaseous products are similarly at high pressure, and mechanical work can be extracted from the high-pressure gas in a standard pneumatic actuation fashion. An alternate, more simplistic means of characterizing the decomposition for purposes of pneumatic actuation is to consider the reaction as a volumetric flow rate amplifier (resulting from the extreme change in density). Although the gain of this amplifier depends upon the downstream pressure, at atmospheric pressure and assuming a 100% concentration of peroxide, this gain would be approximately 6600.

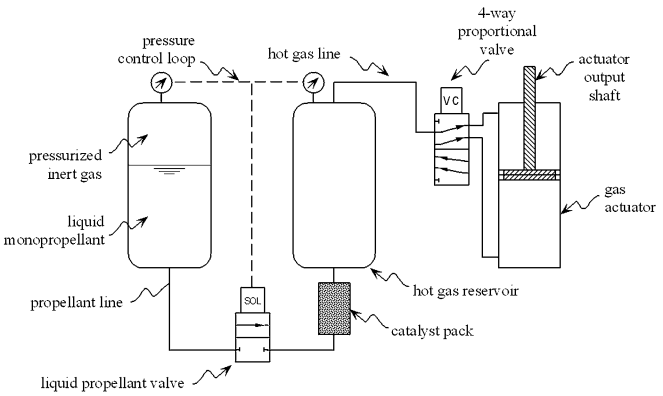

Fig. 1. Schematic of monopropellant-based actuation system.

A schematic drawing of the proposed actuation system is shown in Fig. 1. The conversion of stored chemical energy to controlled mechanical work takes place as follows. The liquid H_2O_2 is stored in a tank pressurized with inert gas (called a blowdown tank) and metered through a catalyst pack by a solenoid-actuated control valve. Upon contact with the catalyst, the peroxide expands into oxygen gas and steam. The flow of peroxide is controlled to maintain a constant pressure in the reservoir, from which the gaseous products are then metered through a voice-coil-actuated four-way proportional spool valve to the actuator. Once the gas has exerted work on its environment, the lower energy hot gas mixture is exhausted to atmosphere.

III. Monopropellant Actuator Prototype

A. Hardware

A prototype of the monopropellant-powered actuation system depicted in Fig. 1 was fabricated and integrated into a single-degree-of-freedom manipulator, as shown in Fig. 2. The primary objective of building the prototype was to demonstrate tracking control and to conduct experiments characterizing the actuation potential described by (1). The propellant is stored in a stainless-steel blowdown propellant tank, and is metered through a two-way solenoid-actuated fuel valve (Parker/General Valve Series 9) through a catalyst pack and into a stainless-steel reservoir. The catalyst pack was constructed in house and consists essentially of a 5-cm-long (2 in), 1.25-cm-diameter

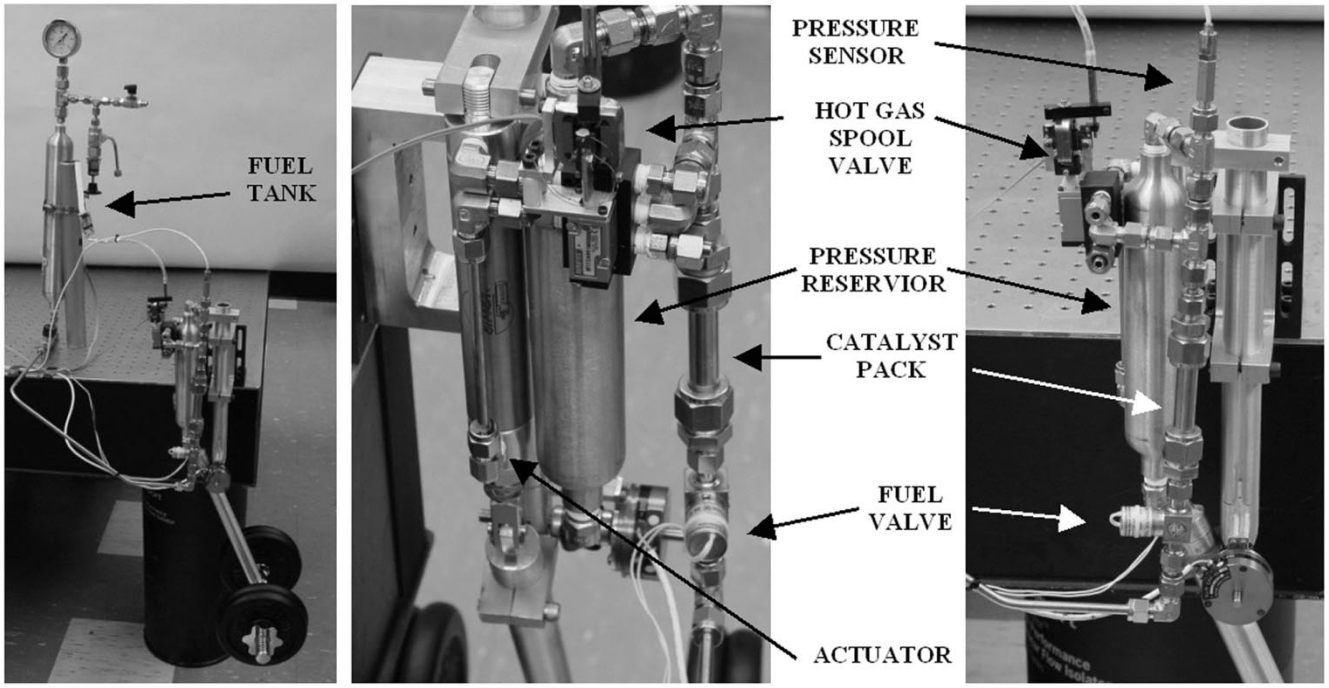

Fig. 2. Single-degree-of-freedom manipulator with monopropellant-based actuation prototype.

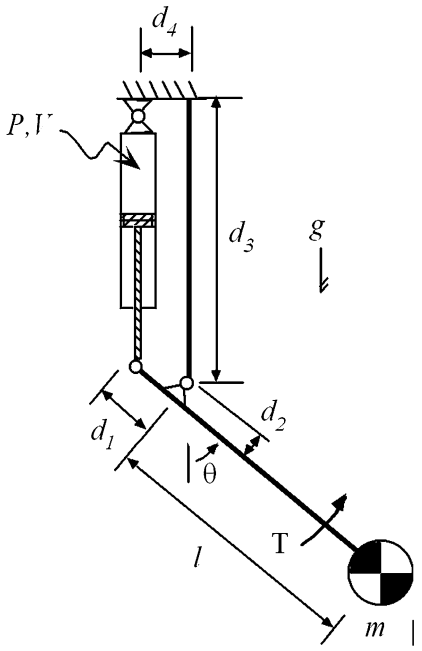

Fig. 3. Kinematic diagram of single-degree-of-freedom manipulator.

(0.5 in) stainless-steel tube packed with catalyst material. A pressure sensor (Kulite model XTME-190-250A) measures the reservoir pressure for purposes of pressure regulation. The high-pressure hot gas is metered into and out of a 2.7 cm (1-1/16 in) inner diameter, 10 cm (3.9 in) stroke double-acting single-rod cylinder (Bimba model 094-DX) by a four-way spool valve (Numatics Microair model #M11SA441M), modified for proportional operation by replacing the solenoid actuator with a thermally isolated voice coil (BEI model #LA09-10-000A). The valve spool displacement is measured with a differential variable reluctance transducer (DVRT) (Microstrain model #2247-6) in order to enable closed-loop control of the valve spool position. The pneumatic cylinder is kinematically arranged to produce a bicep-curling motion upon extension of the piston, as illustrated in Fig. 3.

B. Control

Control of the system is achieved using three separate control loops. The first and simplest is the pressure regulation of the reservoir. Pressure feedback from the pressure sensor switches the solenoid fuel valve with a thermostat-type on-off controller that regulates the reservoir pressure to 1515 kPa (220 psig). The second control loop provides a high-bandwidth (i.e., approximately 10 Hz) position control of the valve spool. Specifically, the DVRT provides position feedback for a proportional-integral-derivative (PID) controller with feedforward Coulomb friction compensation that positions the spool by means of the voice coil actuator. Finally, the valve spool position is commanded by an outer control loop, which controls the angular motion of the single-degree-of-freedom manipulator. The outer control loop utilizes a rotary potentiometer to provide arm angle measurement for a position, velocity, acceleration (PVA) feedback controller, which, as previously mentioned, commands the valve spool position. These control loops were all implemented at a sampling rate of 1 kHz with the real-time interface provided by MATLAB/Simulink (The MathWorks, Inc.). Tracking performance of the manipulator is demonstrated by the data shown in Figs. 4 and 5, both of which reflect tracking with an 11-kg (25 lb) endpoint mass (as shown in Fig. 2) and 70% hydrogen peroxide solution (i.e., diluted with 30% water by weight). Specifically, Fig. 4 shows 30-degree amplitude, 1-Hz

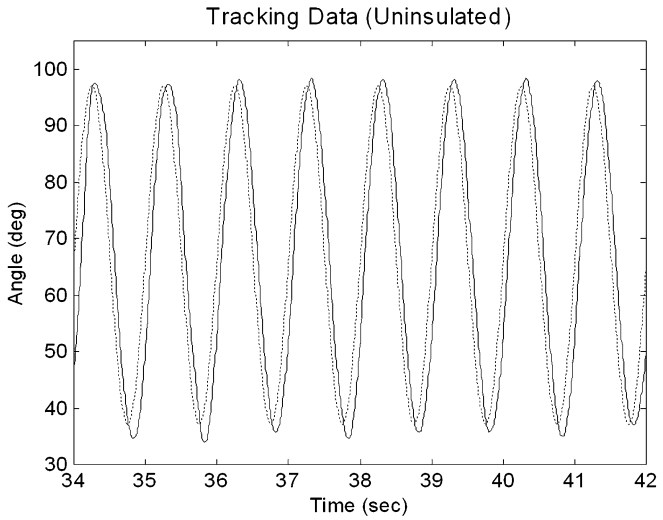

Fig. 4. Closed-loop tracking control of a 30-degree-amplitude 1-Hz sinusoid. The dashed line is the commanded input and the solid is the manipulator motion.

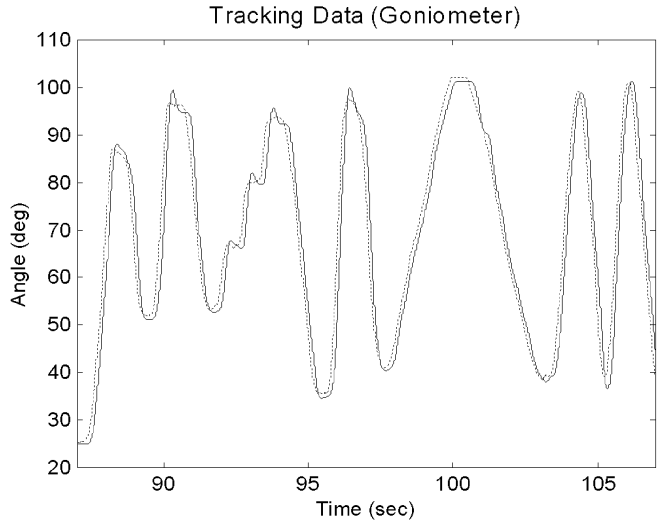

Fig. 5. Closed-loop tracking control of arbitrary human movement. The dashed line is the commanded input and the solid is the manipulator motion.

sine wave tracking, and Fig. 5 shows tracking of an arbitrary input, which was generated by measuring human elbow motion with a goniometer.

IV. Energetics

As previously mentioned, one of the primary objectives in developing a prototype was to evaluate the energetic properties of the system, and in particular to measure the actuation potential as given by (1). Since the thermodynamic energy density of the propellant is known and the conversion system mass can be measured, calculation of the actuation potential primarily requires measurement of energy conversion efficiency, from the energy released as heat to that delivered as controlled mechanical work. In order to determine an upper bound for the conversion efficiency, and to place the experimental results in context, a thermodynamic model was initially developed to estimate the conversion efficiency.

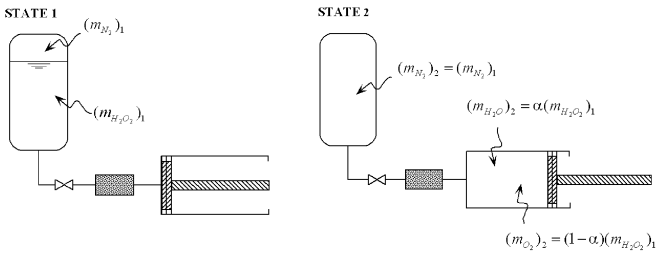

Fig. 6. Thermodynamic states for modeling actuation efficiency.

A. Thermodynamic Modeling

A simplified schematic of the idealized energy conversion process is shown in Fig. 6. In the schematic, state 1 (shown on the left) represents the system containing some bolus of unreacted propellant. State 2 (shown on the right) depicts the system at some later point in time when the bolus of propellant shown in state 1 has been entirely reacted (though not yet exhausted), and through its expansion has performed some work on the environment by means of the pneumatic piston. Assuming, for purposes of establishing an upper bound on efficiency, that no heat loss occurs during the process, the work performed on the load between states 1 and 2 will result directly in a decrease in the internal energy of the propellant, such that

$$U_2 - U_1 = -\int_1^2 P\,dV \tag{2}$$

where U_i is the internal energy of the propellant in state i, and the integral represents the work done by the gas/piston system to the surroundings, following the typical thermodynamic sign convention of positive work associated with an increase in system volume. The left-hand side of (2) can be expressed by mass fractions and mass-specific internal energy states as

$$\begin{aligned} U_2 - U_1 = {} & (m_{\mathrm{H_2O}})_2(u_{\mathrm{H_2O}})_2 + (m_{\mathrm{O_2}})_2(u_{\mathrm{O_2}})_2 \\ & + (m_{N_2})_2(u_{N_2})_2 - (m_{\mathrm{H_2O_2}})_1(u_{\mathrm{H_2O_2}})_1 \\ & - (m_{N_2})_1(u_{N_2})_1 \end{aligned} \tag{3}$$

where $(m_A)_i$ and $(u_A)_i$ are the mass and mass-specific internal energy, respectively, of species A in state i. This expression can be further reduced by assuming that the energy contributed by the nitrogen gas used to pressurized the propellant tank is small (which is indeed the case), so that all nitrogen terms are dropped from the expression. Further, noting that enthalpy is defined as

$$h = u + Pv \tag{4}$$

where P is pressure and v is specific volume, the internal energy of the liquid propellant can be rewritten in terms of its enthalpy, pressure, and specific volume. Additionally, if the mass fraction of water in the reaction products (which is a function of the peroxide concentration in the propellant solution) is defined as

$$\alpha = \frac{(m_{\mathrm{H_2O}})_2}{(m_{\mathrm{H_2O_2}})_1} \tag{5}$$

then, the mass terms of (3) can be rewritten as a function solely of the propellant mass. Finally, in order to evaluate the expression, the specific internal energies and enthalpies must

be expressed relative to reference states, which results in the following restatement of (3)–(5):

$$\begin{aligned} U_2 - U_1 = (m_{H_2O_2})_1 \{&\alpha[(u_{H_2O})_2 - (u_{H_2O})_0] \\ &+ (1-\alpha)[(u_{O_2})_2 - (u_{O_2})_0] + \alpha(h_{H_2O})_0 \\ &+ (1-\alpha)(h_{O_2})_0 - (h_{H_2O_2})_1 - \alpha(Pv_{H_2O})_0 \\ &- (1-\alpha)(Pv_{O_2})_0 + (Pv_{H_2O_2})_1\} \end{aligned} \quad (6)$$

where the subscript 0 denotes the reference state. Note that all terms on the right-hand side of (6) are available as functions of temperature and/or pressure in their respective state, including the mass of the propellant, which is given by

$$(m_{H_2O_2})_1 = (m_{H_2O})_2 + (m_{O_2})_2 = \frac{P_2V_2}{RT_2} \quad (7)$$

where R is the specific gas constant of the state 2 mixture of oxygen and steam, and P_2, V_2, and T_2 are the pressure, volume, and temperature, respectively, in the final state (state 2). Note that since all initial conditions are known, and since the final pressure and volume will be a function of the load profile and device kinematics, (6) is expressible as a function of only final temperature (T_2). Note also that this expression cannot be written explicitly, since the internal energies and enthalpies in (6) cannot be assumed to be expressible as functions of constant specific heats, and therefore must be found in thermodynamic property tables. See references [2] and [3] for steam and oxygen tables, respectively.

As described by (6), the left-hand side of (2) is a function of the thermodynamics of the propellant and its reaction products. Unlike the left-hand-side, the right-hand side of (2) is a function solely of the load profile, or more specifically, a function of the load and the trajectory. For the analysis described by Fig. 6, the trajectory (or trajectory segment) should be a monotonically increasing motion, since gas can be released into the cylinder but not exhausted. In an actual system, a double-acting cylinder would be utilized to provide motion in both directions. For this analysis and for the experiments characterizing the actuation potential of the actuation system described by Fig. 3, a sinusoidal trajectory of the 11 kg (25 lb) load mass through gravity was assumed to be a representative load profile for a human-scale robot. Such a trajectory is characterized by

$$\theta(t) = A\sin\omega t + C \quad (8)$$

where θ is the (elbow) joint angle (see Fig. 3), A is the amplitude of motion, ω is the frequency of motion, and C is angle offset. This load and trajectory would require a joint torque profile given by

$$\tau(\theta) = ml^2\omega^2(C-\theta) + mgl\sin\theta \quad (9)$$

where m is the mass of the load inertia, l is the radius of gyration, and g is gravity as depicted in Fig. 3. The right-hand side of (2) can therefore be written as

$$\begin{aligned} -\int_1^2 P\,dV &= -\int_{\theta_1}^{\theta_2} \tau(\theta)\,d\theta \\ &= \left[\frac{ml^2\omega^2}{2}\theta^2 - ml^2\omega^2C\theta + mgl\cos\theta\right]_{\theta_1}^{\theta_2} \end{aligned} \quad (10)$$

TABLE I
MODEL PARAMETERS CHARACTERIZING EXPERIMENTAL SETUP

Parameter	Value
Pressure in tank (P_1)	1500 kPa
Temperature in tank (T_1)	25°C
Mass fraction (α)	0.67
Initial angle (θ_1)	38 deg
Final angle (θ_2)	98 deg
Load mass (m)	11 kg
Sinusoidal frequency (ω)	2π rad/sec
Arm length (l)	28 cm
Arm geometry: d_1	5.6 cm
Arm geometry: d_2	2.5 cm
Arm geometry: d_3	27 cm
Arm geometry: d_4	5.0 cm

where θ_1 and θ_2 characterize the envelope of the sinusoidal motion. Note that A and C of (8) are expressible in terms of θ_1 and θ_2. Since all terms on the right-hand-side of (10) are known, the only unknown quantity in (2) is the final temperature, T_2. Equations (2)–(10) can therefore be solved for T_2, which yields the required mass of propellant from (7).

The efficiency of conversion is thus found from the combination of the known output work (10), the known required propellant mass (7), along with the energy density of the power source, e_s (which in this case is 2.0 MJ/kg and is the mass specific heat of decomposition of 70% H_2O_2 obtained from a reference such as [4])

$$\eta = \frac{-\int_1^2 P\,dV}{(m_{H_2O_2})_1 e_S}. \quad (11)$$

Given the kinematics of Fig. 3 and the use of a 70% hydrogen peroxide solution, the conversion efficiency was calculated based upon (2)–(11) and the parameters listed in Table I. The total amount of mechanical work performed during the stated trajectory (i.e., in lifting the weight), as given by (10), is 28.7 J, which results in a final temperature of $T_2 = 157$ °C, as calculated from (2)–(7), and requires a total propellant mass of $(m_{H_2O_2})_1 = 0.09$ g as given by (7). The resulting conversion efficiency is $\eta = 16.0\%$, as given by (11). Note that the parameters used in the calculation are reflective of those used in the experiment in the following section. Note also that a 70% propellant solution was utilized in the experiments (and calculation) because it is the highest concentration with which commercial pneumatic components can be used. Higher concentrations result in higher temperatures, which will melt the seals in commercially available pneumatic components. Finally, it should be noted that the efficiency of conversion is derived assuming an energy density based upon a 2.0 MJ/kg heat of decomposition for 70% H_2O_2, which assumes liquid water as a product of the decomposition process. Since the actuator relies on gas as an energetic medium, and since the actuation system is not designed to utilize energy resulting from condensation of the steam (steam quality less than 100%), the energy required to vaporize the water will not be recovered and as a result the conversion efficiency is lower than if state 2 included partial condensation.

The best possible efficiency would occur when partial condensation is allowed to occur within the actuator and also when the load profile of the piston is tailored to allow isentropic expansion from high pressure (P_1) down to the lowest pressure possible for P_2 (atmospheric pressure). In particular the most efficient load profile is such that the expansion of the peroxide reaction products is isobaric until all propellant mass is in the actuator, at which point the expansion becomes isentropic and continues as such until the cylinder pressure reaches atmospheric. Partial condensation occurs as a result of this load profile, leaving 70% quality steam in the actuator. This load profile would yield a theoretical efficiency of $\eta = 39\%$ for the 70% peroxide solution at a supply pressure of 220 psig. Viewed in this sense, an efficiency of 16%, based on the load profile specified in Table I, is nearly half of the maximum possible for a 70% peroxide solution.

B. Uninsulated Experiments

Experiments were conducted to measure the previously calculated conversion efficiency. As previously mentioned, a 70% peroxide solution was used as the propellant to maintain acceptable temperatures for commercially available components. For these experiments, the single-degree-of-freedom manipulator was commanded to move the 11 kg mass through a 30-degree amplitude, 1-Hz sinusoidal motion enveloped by initial and final angles of $\theta_1 = 38^\circ$ and $\theta_2 = 98^\circ$, respectively, defined relative to the downward vertical as depicted in Fig. 3. The work output was computed indirectly by measuring the angle and, in post-processing, computing the actuation torque using a model of the load, given by

$$\tau = ml^2\ddot{\theta} + mgl\sin\theta. \tag{12}$$

The instantaneous power could then be calculated as

$$\mathbf{P}(t) = \left|\tau\dot{\theta}\right|, \tag{13}$$

where the absolute-value operator reflects the fact that typical spool-valve controlled systems are energetically nonconservative. The average power was calculated by integrating over an integer number of cycles n

$$\mathbf{P}_{\text{ave}} = \frac{\int_{t_1}^{t_2}\mathbf{P}(t)\,dt}{t_2 - t_1} \tag{14}$$

where $\omega(t_2 - t_1) = 2\pi n$. The propellant mass consumption was measured indirectly by recording the pressure of the nitrogen gas in the blowdown tank, assuming an isothermal process inside the constant-volume tank, and calculating the volume occupied by the nitrogen from the ideal gas equation, which in turn yields the volume of propellant in the tank. Since the propellant is a liquid, the mass of propellant used $m_{\text{H}_2\text{O}_2}$ is easily computed from the known volume and density. The conversion efficiency is then computed over an integer number of cycles as follows:

$$\eta = \frac{\mathbf{P}_{\text{ave}}(t2 - t1)}{e_S m_{\text{H}_2\text{O}_2}} \tag{15}$$

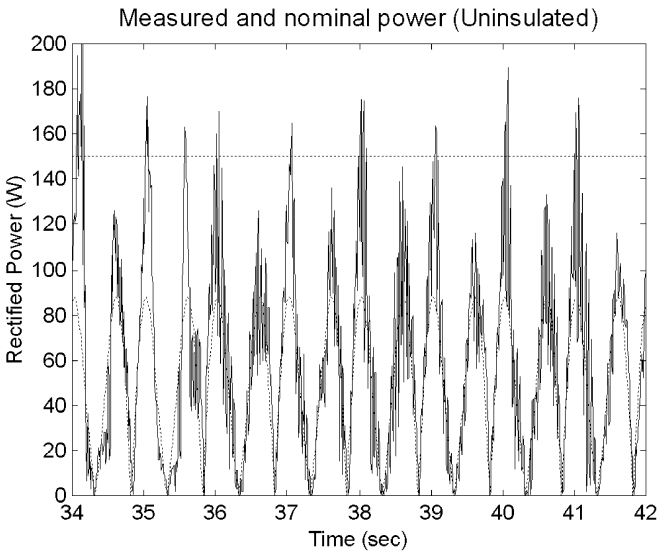

Fig. 7. Comparison of the measured power delivered by the actuator (solid) to the theoretically predicted power (dashed) required to track the specified angular trajectory of the arm. Also shown is the estimated peak power (also dashed).

where e_S is again the heat of decomposition of 70% hydrogen peroxide solution. Based on these measurements, the experimentally determined conversion efficiency was found to be $\eta = 6.6\%$. Note that the electrical power required to operate the valves was neglected in this analysis. The measured average combined electrical power required by the fuel and gas valves was approximately 2 W. Since this is only about 3% of the average work delivered by the actuator, this electrical power can be legitimately omitted from the analysis.

The significant discrepancy between the measured conversion efficiency of 6.6% and the calculated upper bound of 16% is due to two major factors. The first is inefficiency in control and the second is heat loss. Specifically, the thermodynamic model assumed that no gas was exhausted during a given monotonic segment of the trajectory, and that no energy was lost as heat. Regarding the former, any overshoot of the desired trajectory will violate the assumed monotonicity of the trajectory, and therefore will result in an intermittent exhaust of hot gas and a resulting decrease in the efficiency. The existence of such intermittent exhaust is evident in the oscillations exhibited in the power delivered to the load, computed from (12) and (13), which is shown in Fig. 7 plotted against the theoretically required power, computed from (8) and (9).

Regarding inefficiency due to heat loss, the external surfaces of the catalyst pack, reservoir, and actuator were hot during the experiments, thus indicating the presence of heat flow. In order to more quantitatively assess the degree of heat loss, the prototype was instrumented with thermocouples so that the rate of heat loss could be estimated from surface temperature measurements referenced to tables associated with heat loss from uninsulated steam piping [5]. This measurement yielded an estimated heat loss rate of 140 W. Note that the average measured mechanical power output was approximately 60 W. The prototype lost twice as much energy in the form of heat as it delivered in the form of work. The decrease in efficiency due to heat loss

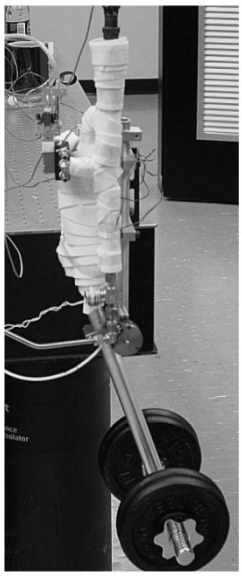

Fig. 8. Monopropellant actuator prototype wrapped with insulating tape and instrumented with thermocouples for measurement of surface temperature.

is easily accounted for in the thermodynamic model by simply altering (2) to include a heat-loss term

$$U_2 - U_1 = Q_{1\to 2} - \int_1^2 P\,dV \tag{16}$$

where $Q_{1\to 2}$ is the heat loss, calculated by measuring the average heat loss rate as previously described, and multiplying by the duration of the experiment. For the experimental conditions described by Table I, and with an average heat loss rate of 140 W, the conversion efficiency was recalculated to be $\eta = 10.0\%$, as compared to the measured value of $\eta = 6.6\%$. Having accounted for the heat loss, the remaining discrepancy is presumably due to the closed-loop control inefficiency, which is not so easily accounted for in the thermodynamic model.

C. Insulated Experiments

In order to improve the measured conversion efficiency, the catalyst pack, reservoir, and actuator were wrapped in insulating tape, as shown in Fig. 8, and measurement of the conversion efficiency was repeated. For the insulated case, the experimentally determined conversion efficiency was found to be $\eta = 9.0\%$. Thermocouple measurement of the surface temperatures, as previously described, yielded an estimated heat loss rate of 73 W, approximately half of the uninsulated case. Using this heat loss rate, the theoretically calculated efficiency was $\eta = 12.0\%$, the difference presumably due to control inefficiency (i.e., intermittent exhausts).

D. Experimentally Determined Actuation Potential

Having measured the conversion efficiency, the mass-specific power density of the actuator and the mass-specific energy density of the power source need to be determined in order to calculate the actuation potential (1). The former is found by determining the mass and the maximum output power of the energy conversion and actuation system. Though finding the mass is a trivial task, characterizing the maximum deliverable power is not as straightforward, in large part due to the dependence upon several factors, including the supply pressure, the valve flow coefficient (C_v) of the proportional valve, and the nature of the load, among others. In order to base the actuator power density solely on measured data, the authors chose to conservatively estimate the maximum deliverable power by using the peak power consistently measured during the previously described efficiency experiments. As evidenced by the data in Fig. 7, the actuator can consistently generate peak power of 150 W, as indicated by the dashed line overlaid on the plot. The mass of the actuation system was obtained by weighing the components of the actuator shown in Fig. 2. The mass of each component is summarized in Table II. As indicated in the table, the total actuation system mass is 1.5 kg, thus resulting in an actuation system power density of $p_a = 100$ W/kg. This would increase for a multi-degree-of-freedom system, since such a system would only include a single fuel valve, catalyst pack, pressure reservoir, and pressure sensor.

TABLE II
MASS OF ACTUATOR COMPONENTS

Actuation Component	Mass (g)
Proportional spool valve	215
Pressure sensor	35
Fuel valve	90
Catalyst pack	200
Reservoir tank	430
Pneumatic cylinder	230
Fittings	300
TOTAL ACTUATOR	**1500**

Having determined the actuator power density, only the power-source energy density need be found in order to calculate the actuator potential. As previously mentioned, the heat of decomposition of 70% hydrogen peroxide propellant is 2.0 MJ/kg. The propellant must be stored, however, in a pressurized blowdown propellant tank, and as such a legitimate characterization of the energy density should include the mass of a tank. Based on available data for a composite overwrapped propellant tank [6], the mass of a propellant tank for a volume on the order of 10 liters would conservatively decrease the mass-specific energy density of 70% peroxide from approximately 2.0 MJ/kg to approximately 1.7 MJ/kg. Based on this and the measured values of conversion efficiency and actuator power density previously described, the actuation potential for this single-degree-of-freedom system, as given by (1), would be $A_p = 15.3$ kJ·kW/kg^2. As previously mentioned, the power density will increase for a multi-degree-of-freedom system, and thus so will the actuation potential. For a six-degree-of-freedom system, for example, the total actuation system mass would be 5.2 kg, or 870 g per actuator. Note that the reservoir used in the single-degree-of-freedom experiment was oversized, and is appropriately sized for a power-comparable six-degree-of-freedom system. The actuation system power density would therefore increase to $p_a = 172$ W/kg, and the corresponding actuation potential to $A_p = 26.4$ kJ·kW/kg^2 for the six-degree-of-freedom system.

For purposes of comparison, the best commercially available rechargeable batteries have energy densities of approximately 180 kJ/kg (e.g., Evercel M40-12 nickel zinc, or SAFT 27 × 10 LAS silver zinc). A rare-earth permanent-magnet dc motor with a harmonic drive gearhead with output characteristics capable of achieving the trajectory specified by Table I, has a power density of approximately 48 W/kg (e.g., Kollmorgen model N12M4 Neodymium Servodisc motor with Harmonic Drive Technologies PSS-G20-100 gearhead). Note that this remains invariant, regardless of the number of degrees of freedom. Finally, one can assume that the overall conversion efficiency would be the combined efficiencies due to pulsewidth-modulation (PWM) control, the motor, and the gearhead. The PWM efficiency was estimated to be 95%, the motor efficiency calculated for the desired trajectory to be 90% (i.e., the resistive power loss in the motor windings was calculated given the desired torque), and the harmonic drive gearhead efficiency was estimated based on manufacturer data to be 65%. The resulting actuation potential for this type of system would therefore be $A_p = 4.8$ kJ·kW/kg^2. The poorly insulated single-degree-of-freedom experimental setup with 70% peroxide therefore exhibited an actuation potential more than three times a state-of-the-art battery/dc motor system. A similar six-degree-of-freedom system would exhibit an actuation potential over fives times the battery/dc motor system.

E. Projected Performance for High-Test Propellant

Though improvements can clearly be made with improved insulation and control performance, the most obvious means of improving the actuation system performance is to substitute a fully concentrated version of the propellant (i.e., 100% hydrogen peroxide) in place of the 70% solution used in the previously described experiments. Though procedurally quite simple, such experiments cannot be performed on commercially available pneumatic components, due to the high decomposition temperatures. Specifically, the adiabatic decomposition temperature of 100% peroxide is approximately 1000 °C (1800 °F), compared to approximately 230 °C (450 °F) for a 70% solution [4]. Rather than conducting experiments using 100% peroxide, one can obtain a reasonable estimate of performance with projections based upon the experiments conducted with 70% solution. Upon replacing 70% propellant with 100% (technically 99.6%), at least two of the three parameters forming the actuation potential figure of merit would be expected to increase. Specifically, since the propellant contains more peroxide per unit mass, the heat of decomposition increases by a factor of 1.45 from 2.0 MJ/kg to 2.9 MJ/kg [4]. Additionally, recall that the relatively low conversion efficiencies described in Section IV-A were primarily due to the heat required to vaporize the water in the reaction product. Since the 100% propellant contains less water, less energy is invested in vaporizing the reaction product. Recalculating the expected efficiencies accounting for the reduced water content, the conversion efficiency scales by a factor of 1.56. Assuming that the actuation system power density remains invariant (i.e., that it does not increase with the 100% propellant), the single-degree-of-freedom system shown in Fig. 2 with 100% propellant would be expected to have an actuation potential of $A_p = 35.0$ kJ·kW/kg^2, which is 7.3 times greater than the battery/dc motor system. A similar six-degree-of-freedom system would exhibit an actuation potential of $A_p = 60.4$ kJ·kW/kg^2, more than an order of magnitude greater than the battery/dc motor system. The promise of such performance, which would presumably be further improved with better insulation and lightweight components, justifies the fabrication of custom high-temperature pneumatic components.

V. Conclusion

A power supply and actuation system appropriate for a position or force controlled human-scale robot was proposed. The proposed approach utilizes a monopropellant as a gas generant to power pneumatic-type hot gas actuators. Experiments were performed that characterize the energetic behavior of the proposed system and offer the promise of an order-of-magnitude improvement in actuation potential relative to a battery-powered dc-motor-actuated approach. Experiments also demonstrated good tracking and adequate bandwidth of the proposed actuation concept.

References

[1] D. H. Morash, "Hypergolic/catalytic actuator," U.S. Patent 4 825 819, May 2, 1989.

[2] J. H. Keenan, F. G. Keyes, P. G. Hill, and J. G. Moore, *Steam Tables*. New York: Wiley, 1969.

[3] M. W. Chase, Jr., C. A. Davies, J. R. Downey, Jr., D. J. Frurip, R. A. McDonald, and A. N. Syverud, "JANAF thermochemical tables third edition," *J. Phys. Chem. Ref. Data*, vol. 14, Suppl. 1, 1985.

[4] L. H. Dierdorff *et al.*, *Hydrogen Peroxide Physical Properties Data Book*, 2nd ed. Buffalo, Ny: Becco Chemical Division, FMC Corporation, 1954.

[5] R. A. Parsons, Ed., *ASHREA Handbook: Fundamentals*, I-P ed. Atlanta, GA: American Society of Heating, Refrigerating and Air-Conditioning Engineers, Inc., 1993.

[6] W. H. Tam, I. A. Ballinger, J. Kuo, W. D. Lay, S. F. McCleskey, P. Morales, Z. R. Taylor, and S. J. Epstein, "Design and manufacture of a composite overwrapped xenon conical pressure vessel," in *Proc. 32nd AIAA/ASME/SAE/ASEE Joint Propulsion Conf.*, Lake Buena Vista, FL, July 1–3, 1996, Paper AIAA 96-2752.

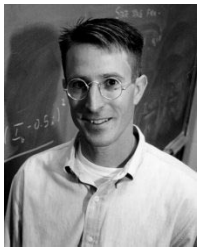

Michael Goldfarb (M'94) received the B.S. degree in mechanical engineering from the University of Arizona, Tucson, in 1988, and the M.S. and Ph.D. degrees in mechanical engineering from the Massachusetts Institute of Technology, Cambridge, in 1992 and 1994, respectively.

In 1994, he joined the Department of Mechanical Engineering at Vanderbilt University, Nashville, TN, where he is currently an Associate Professor. His current research interests include the design of high-energy-density robotic actuators, the control of fluid-powered actuators, and the design and control of haptic interfaces and telemanipulator systems.

Eric J. Barth (M'00) received the B.S. degree in engineering physics from the University of California at Berkeley, and the M.S. and Ph.D. degrees from the Georgia Institute of Technology, Atlanta, all in mechanical engineering in 1994, 1996, and 2000, respectively.

He is currently an Assistant Professor of Mechanical Engineering at Vanderbilt University, Nashville, TN. His research interests include the design, modeling and control of mechatronic systems, actuator development for autonomous robots, control of fluid power systems, multiagent robotic systems, and applied nonlinear control.

Michael A. Gogola received the Bachelor's degree in mechanical engineering from Michigan State University, East Lansing, in 1996 and the Master's degree in mechanical engineering from Vanderbilt University, Nashville, TN, in 1998.

He was a Research Engineer in the Department of Mechanical Engineering at Vanderbilt University and is currently a Mechanical Design Engineer for Baker Hughes INTEQ, Houston, TX, working on the design of oil drilling and evaluation technology.

Joseph A. Wehrmeyer received the B.S. and M.S. degrees in engineering from Southern Illinois University, Carbondale, IL, in 1981 and 1986, respectively, and the Ph.D. degree in mechanical engineering from Vanderbilt University, Nashville, TN, in 1990.

Before returning to Vanderbilt in 1997 as a Research Associate Professor, he worked at both the University of Missouri-Columbia and the NASA Marshall Space Flight Center, Huntsville, AL. His current research interests include the use of propellants, traditionally used for rocket propulsion, for other innovative applications.